

# MICROSCALE ISOTOPIC DIVERSITY OF MACROMOLECULAR ORGANIC MATTER FROM ASTEROID RYUGU. J. Barosch<sup>1\*</sup>, L. R. Nittler<sup>1</sup>, B. T. De Gregorio<sup>2</sup>, R. M. Stroud<sup>2</sup>, H. Yabuta<sup>3</sup>, and the Hayabusa2-initial-analysis IOM team, H. Yurimoto<sup>4</sup>, T. Nakamura<sup>5</sup>, T. Noguchi<sup>6</sup>, R. Okazaki<sup>7</sup>, H. Naraoka<sup>7</sup>, K. Sakamoto<sup>8</sup>, S. Tachibana<sup>9</sup>, S. Watanabe<sup>10</sup> and Y. Tsuda<sup>8</sup>

<sup>1</sup>Carnegie Institution of Washington, Washington DC, USA (\*jbarosch@carnegiescience.edu). <sup>2</sup>US Naval Research Laboratory, Washington DC, USA, <sup>3</sup>Hiroshima Univ., <sup>4</sup>Hokkaido Univ., <sup>5</sup>Tohoku Univ., <sup>6</sup>Kyoto Univ., <sup>7</sup>Kyushu Univ., <sup>8</sup>ISAS, JAXA, <sup>9</sup>Univ. of Tokyo, <sup>10</sup>Nagoya Univ.

**Introduction:** Primitive solar system objects such as chondrites, interplanetary dust particles and comets contain macromolecular organic matter (MOM). This material is a major carrier of H, C, N and noble gases and probably a significant source of these elements and of prebiotic molecules on Earth [1]. However, its origin and formation mechanism(s) are still debated. It is also unclear to what degree the organic matter was modified by heating and/or aqueous alteration on the parent bodies.

A key goal of the Hayabusa2 sample-return mission is to understand the nature and origin of organic matter in asteroid (162173) Ryugu. We used the Carnegie NanoSIMS 50L to investigate the H, C and N isotopic composition of organic matter in Ryugu particles. We compare our results to the compositions and characteristics of organic matter in primitive chondrites and determine similarities and differences. We also detected rare presolar SiC grains in the Ryugu samples, discussed separately [2].

**Samples and Methods:** We prepared a total of 9 Ryugu grains for NanoSIMS analyses. Four grains from chamber A (A0108-8, -9, -11, -14; collected during the first touchdown) and three grains from chamber C (C0109-8, -11, -19; collected during the second touchdown) were embedded in S and sectioned with an ultramicrotome. The ~250 nm thick slices were deposited onto Si wafers and the S sublimated overnight in a 60 °C oven. Adjacent thin sections of the same grains were kept for coordinated analysis by transmission electron microscopy (TEM) [3] and synchrotron X-ray microscopy (STXM) [4].

One grain from chamber A (A0108-13) and one grain from chamber C (C0109-2) was crushed between glass slides. A few dozen ~15–30 µm-sized particles were extracted with a micromanipulator and pressed with quartz disks into annealed gold foils to produce flat grain surfaces.

We first analyzed C and N isotopes (as <sup>12</sup>C<sub>2</sub>, <sup>12</sup>C<sup>13</sup>C, <sup>12</sup>C<sup>14</sup>N, and <sup>12</sup>C<sup>15</sup>N, plus <sup>16</sup>O, <sup>28</sup>Si, <sup>32</sup>S or MgO and secondary electrons) using a ~0.4 pA, ~100-nm Cs<sup>+</sup> primary beam. All samples were then re-analyzed for <sup>1</sup>H, D, and <sup>12</sup>C isotopes, as well as secondary electrons. We used the same magnification and increased the primary beam current to ~1.2 pA (size <200 nm). Some sections were subsequently re-measured for C and N

isotopes to improve the counting statistics and an electron gun was used for some measurements to prevent charging. Total counting times varied between ~0.1 s/0.01 µm<sup>2</sup> for each run. C-rich regions of interest (ROIs) were defined in the C-N images and subsequently relocated in the H-D images. Due to sputtering of material, not all ROIs were present in both sets of images. Terrestrial and meteoritic samples were used as isotopic standards.

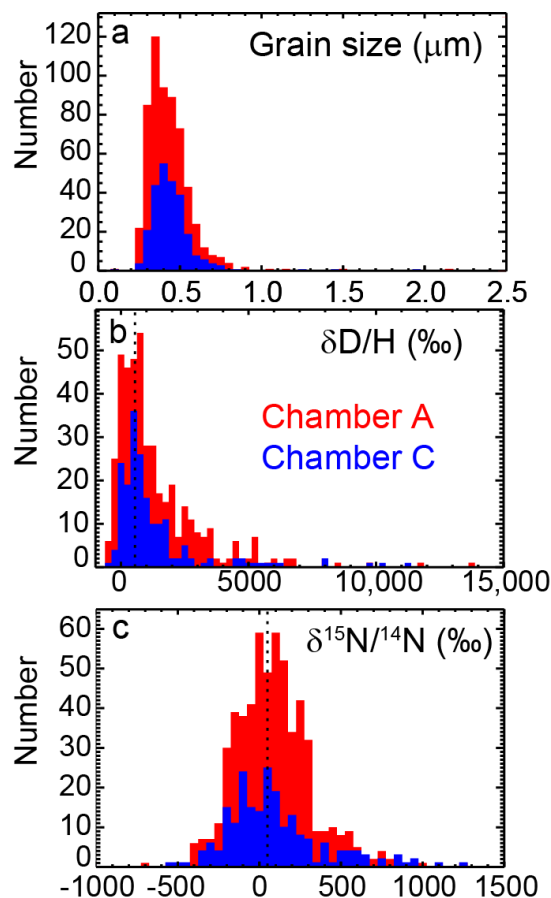


**Fig. 1:** Histograms of a) grain size, b)  $\delta D$ , and c)  $\delta^{15}N$  in ~900 C-rich ROIs defined in NanoSIMS images of Ryugu particles pressed into Au. Vertical dashed lines indicate approximate average values in b) and c).

**Results and Discussion:** We have thus far determined correlated H, C, and N isotope ratios for ~900 C-rich ROIs in Ryugu grains. Total areas analyzed are 4600 µm<sup>2</sup> in chamber A grains and 1800 µm<sup>2</sup> in

chamber C grains. We focus here mostly on the analyses of pressed particles as these are less susceptible to terrestrial contamination than the microtomed samples. Most defined ROIs range from ~200 to 700 nm in size (Fig. 1a), but some range up to >2  $\mu\text{m}$ . Numerous smaller grains and diffuse C are present as well but are too small for isotopic analysis under our conditions. As seen in MOM from primitive C chondrites [5–9], the Ryugu MOM is, on average, enriched in D (Fig. 1b) and  $^{15}\text{N}$  (Fig. 1c). Most ROIs show compositions consistent within errors with average values of  $\delta\text{D} \sim +600\text{‰}$  and  $\delta^{15}\text{N} \sim 50\text{‰}$ , but 5–10% of the ROIs exhibit much more extreme isotopic enrichments (“hotspots”) or depletions (“coldspots”). Chamber A MOM might have slightly lower  $\delta\text{D}$  and  $\delta^{15}\text{N}$  than chamber C MOM, as seen in Ryugu insoluble organic matter [10], but this may just reflect variable amounts of hotspots in the limited number of analyzed particles.

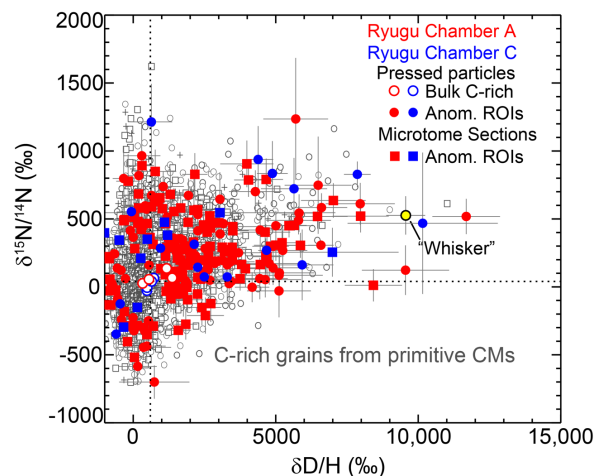


**Fig. 2:** H and N isotopic ratios of Ryugu grains (colored symbols) are compared to those seen in primitive CM chondrites [9]. Dashed lines indicate average values for the Ryugu samples pressed into Au.

Correlated ROI H and N isotopic ratios are shown in Figure 2 and compared with data recently reported for similar measurements in three primitive CM chondrites (grey symbols, [9]). For the Ryugu samples, only bulk (10–30  $\mu\text{m}$ ) particle measurements and hotspot/coldspot (defined as being  $>3\sigma$  different from averages) ROIs are shown. The bulk measurements mostly cluster around average values, though some are strongly affected by one or more hotspots. The Ryugu outliers span very similar ranges to those seen in the CM chondrites. Although many grains are enriched in both D and  $^{15}\text{N}$ , a majority is only anomalous in one or the other isotopic system.

As also seen in meteoritic MOM [11], a very small fraction (~0.5–1%) of the C-rich ROIs were found to have moderate C-isotopic anomalies, typically  $^{13}\text{C}$

enrichments or depletions of order 10–25%, with  $^{13}\text{C}$ -depleted grains generally showing  $^{15}\text{N}$  depletions as well. The NanoSIMS images also revealed sub- $\mu\text{m}$  ROIs with much more extreme  $^{13}\text{C}$  enrichments indicating the presence of presolar SiC grains, discussed in [2].

While the vast majority of the C-rich ROIs appear round in the ion images, we identified one highly unusual rectangular grain in a particle from chamber C (Fig. 3). This “whisker” of approximately  $2.5 \times 0.7 \mu\text{m}$  in size has an extremely anomalous H and N isotopic composition ( $\delta\text{D} = 9,600 \pm 700$ ,  $\delta^{15}\text{N} = 525 \pm 140 \text{‰}$ ; Fig. 2) and among the highest C/H and C/N ratios seen among the C-rich grains. The unique morphology and low H and N contents suggest that this grain may be graphite. Planned Raman measurements may help elucidate the nature and origin of this unusual grain.

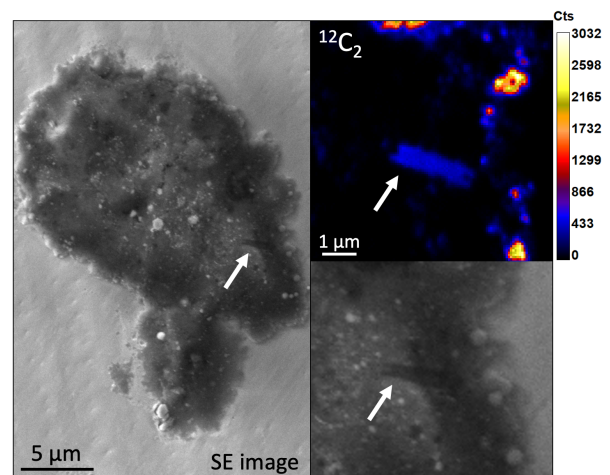


**Fig. 3:** D and  $^{15}\text{N}$ -enriched (graphite?) whisker detected in a particle from chamber C.

**Summary:** We studied correlated H, C, and N isotope compositions of MOM in Ryugu samples. We observed a similar average composition and a similar compositional diversity as seen in chondritic MOM, suggesting similar origin(s) and secondary processing.

**Acknowledgements:** This work was supported by NASA via grants NNX16AK72G (LRN) and 80NSSC20K0340 (LRN).

**References:** [1] Alexander C. M. O’D. et al. (2017) *Chem. Erde* 77, 227–256. [2] Nittler L. R. et al. (2022) *this meeting*. [3] Stroud R. M. et al. (2022) *this meeting*. [4] De Gregorio B. T. et al. (2022) *this meeting*. [5] Busemann H. et al. (2006) *Science* 312, 727–730. [6] Remusat L. et al. (2010) *ApJ* 713, 1048–1058. [7] Nittler L. R. et al. (2019) *Nat. Astron.* 3, 659–666. [8] Nittler L. R. et al. (2018) *GCA* 226, 107–131. [9] Nittler L. R. et al. (2021) *84th MetSoc*, abstr. #6063. [10] Remusat L. et al. (2022) *this meeting*. [11] Floss C. et al. (2009) *ApJ* 697, 1242–1255.